

# Influence of Variation in Combustion Conditions on the Primary Formation of Chlorinated Organic Micropollutants during Municipal Solid Waste Combustion

E. WIKSTRÖM,\* M. TYSKLIND, AND S. MARKLUND

Department of Chemistry, Environmental Chemistry, Umeå University, SE-901 87 Umeå, Sweden

The aim of this study was to investigate the influence of variation in combustion conditions on the primary formation of organic micropollutants (OMPs). The flue gas samples were taken at a relatively high flue gas temperature (650 °C), to enable mechanistic studies on the high temperature formation (primary formation). Eleven experiments were performed in a laboratory scale fluidized bed reactor fed with an artificial municipal solid waste (MSW). The samples were analyzed for mono- to octachlorinated dibenzo-*p*-dioxins and dibenzofurans (CDDs/Fs), tri- to decachlorinated biphenyls (CBs), di- to hexachlorinated benzenes (CBzs), and di- to pentachlorinated phenols (CPhs). In addition to chlorinated OMPs, nonchlorinated dibenzo-*p*-dioxin (DD), dibenzofuran (DF), and biphenyl (BP) were analyzed. The experiments show that variations in the CE influence the degree of chlorination of the organic micropollutants. A correlation between low CE and formation of non- and low-chlorinated OMPs was seen and a distinct relationship of higher chlorinated homologues and efficient combustion condition. Thus, the DiCDFs and DiCBzs are formed during low combustion efficiency (CE), while the PeCDF and PeCBzs formation take place at higher CE. The distribution between primary and secondary air is important for the formation of higher CDDs/Fs and CBzs. The primary formation of CDDs and CDFs is through different mechanisms. The CDDs are mainly formed by condensation of CPhs, while the CDFs are formed through a non- or a low-chlorinated precursor followed by further chlorination reactions.

## 1. Introduction

Several studies have shown a positive correlation between the levels of carbon monoxide (CO) and particulate matter in the flue gas and the formation of chlorinated dibenzo-*p*-dioxins (CDDs) and chlorinated dibenzofurans (CDFs) (1–3). An optimum oxygen level between 7 and 9% for high combustion efficiency and minimization of CDD/F formation has been postulated by Hasselriis et al. (1). Combustion efficiency (CE) is defined as the ratio of organic material oxidized to CO<sub>2</sub>, divided by total organic material oxidized in the process [CE (%) = CO<sub>2</sub>/(CO<sub>2</sub>+CO) × 100]. Nevertheless, the influence of combustion conditions on the formation rate of organic micropollutants (OMPs) is still not fully

established. A correlation between formation of polyaromatic hydrocarbons (PAHs) and low CE has been reported (4); however, the conditions that favor the formation of PAH have been found to suppress the formation of CDD/Fs as well (4, 5). Low levels of CO and/or high oxygen level in the combustion gas are not a guarantee for low OMP emissions or vice versa (4, 6–11). The level of CO in the combustion gas is not the only parameter of importance for the CDD/F emission. The number of periods with CO peaks during the combustion processes has shown to be important as well (2). How the organic compounds are formed is still not completely understood, and many complex formation mechanisms are probably involved in the process. Organic micropollutants, such as CDD/Fs, chlorinated biphenyls (CBs), chlorinated benzenes (CBzs), and chlorinated phenols (CPhs), are formed during combustion of different kinds of fuels. In thermal processes they can be formed either through primary formation, at high temperature (>650 °C), or through secondary formation at lower temperatures (650–250 °C), downstream of the boiler. In the literature two major formation pathways for CDD/Fs are discussed: by thermal decomposition of carbon products which are not completely oxidized (*precursors*) and by *de Novo* synthesis from chlorine, oxygen, hydrogen, and carbon on the fly ash (12–15). A wide range of different products of incomplete combustion are able to act as *precursors* for formation of CDD/F, such as monocyclic aromatics with or without functional groups and aliphatic compounds. The most studied precursor compounds are the chlorinated aromatics (e.g. CPhs and CBzs). Dickson et al. (16) has shown that the two formation mechanisms, *de Novo* and *precursors*, operate independently of each other. The *precursor* mechanism can operate in deficient oxygen conditions or even in a nitrogen (N<sub>2</sub>) atmosphere, while oxygen is essential for formation from carbon (*de Novosynthesis*) (16, 17). It is not established which of these two formation mechanisms that is fastest. It has been shown in several studies that the formation rate of CDDs from CPhs (*precursors*) is faster and that the activation energy of the reaction is lower than for formation through *de Novo* synthesis (16, 18, 19). However, Huang and Buekens (20) declare that the *de Novo* synthesis should be the fastest and most important of these two mechanisms due to much higher levels of carbon than potential precursors in the flue gas. The *de Novo* synthesis, unlike the *precursor* pathway, produces the characteristic (CDF/CCD > 1) ratio in the flue gas (20). On the other hand, it is difficult to separate the two formation mechanisms; Luijl et al. (18) showed that the PCDDs originate directly from the carbon structure of the fly ash by an intermediate chlorophenol structure, i.e. the *de Novo* synthesis acts as a first reaction step for further formation through the *precursor* mechanism. K. Hell (21) et al. found that the PCDFs probably are released from biphenyl structures in the carbon matrix, i.e. a combination between the *de Novo* and the *precursor* mechanism.

The aim with this study was to investigate how the primary formation of CDD/Fs, CBs, CBzs, and CPh is effected by variations in the combustion conditions. This study will focus on the primary formation at high temperature to increase the knowledge of the mechanisms behind the formation of chlorinated organic compounds. Most of the results discussed in the literature consider samples taken after the boiler, i.e. after both primary and secondary reactions. To study the influence of CE variation on the primary formation of OMPs without any effects of secondary formation reactions will give much new information about the mechanisms. To complete the picture of how CDDs/Fs formation is influ-

\* Corresponding author phone: +46-90-786 66 64; fax: +46-90-118 61 55; e-mail: Evalena.wikstrom@chem.umu.se.

enced, the dibenzo-*p*-dioxin (DD), dibenzofuran (DF), and mono- to octachlorinated DD/F were analyzed, and as many congeners as possible were quantified.

## 2. Experimental Section

**2.1. Experimental Setup and Design.** The experiments were performed with an artificial municipal solid waste (MSW) fuel in a 5 kW laboratory scale fluidized bed reactor. The artificial MSW is a mixture of the most important material categories in the waste such as paper, plastic (both polyethylene and poly(vinyl chloride)), wood, kitchen and garden waste, and an incombustible category (glass and metals). The chlorine content of the artificial MSW is 0.67%. The reactor and the composition of the artificial MSW is described in detail elsewhere (22, 23). The main advantages with experiments performed with the reactor and the artificial MSW fuel are that full scale MSW combustor conditions are simulated very well and experiments with inefficient combustion conditions can be performed during controlled conditions. It enables mechanistic studies of OMP formation reactions in complex combustion condition. Further, the reactor is easily cleaned between different experiments in order to minimize the memory effects. In this study, the reactor was fed with 1200 g/h of the artificial MSW fuel, which corresponds to an effect of 5.8 kW. The inorganic gases CO<sub>2</sub>, CO, and O<sub>2</sub> were continuously measured in the flue gas, described by Wikström et al. (23). A flame ionization detector (FID TESTA 123) is continuously measured the level of incomplete combusted total hydrocarbons (THC) in the flue gas. Each combustion experiment consists of one flue gas sample for OMP and one for particulate matter determination in the flue gas. The sample of OMPs was taken directly after the freeboard of the reactor at 650 °C to determine the primary formation of OMPs. The combustion zone where the after burning take place is defined as the freeboard section of the laboratory reactor. Sampling was performed under isokinetic conditions for 45 min, according to a validated method described elsewhere (24, 25). The gas volume was normalized to 1 atm dry gas at 0 °C and 10% CO<sub>2</sub>. The extraction and cleanup procedures for all the compounds studied were performed in agreement to standard methods (26, 27). The CDD/Fs were analyzed with a sector magnetic HRGC/HRMS (VG 70 S, with a Supelco 2330 column), the CBs with HRGC/LRMS (VG 70E-250 with a Supelco 2330 column), and the DD, DF, BP, CPhs, and CBzs with a quadrupole HRGC/LRMS (Fission GC 8000/MD 800, with a J&W DB-5 column). The octaCBs were excluded from the total CB results due to interference in the analysis. The sampling time for particulate matter in the flue gas was 45 min, which corresponds to a flue gas volume of 1.2 nm<sup>3</sup>. The concentration was determined by filtration of the flue gas on hot quartz filter. The experiments in this investigation were planned according to experimental design theory (28). Three factors were selected to be investigated, viz. the total air in to the reactor, distribution of the air between primary and secondary inlet, and the temperature of the secondary air. A complete factorial design (CFD) in two levels was selected for this study (Figure 1). The levels of the three factors in the design are shown in Figure 1, and the actual parameter settings in each experiment are listed in Table 1. All experiments were performed in random order to minimize the effect of systematical errors. To prevent effects of different flue gas residence time due to different total air flow, N<sub>2</sub> was added to a constant flow of 150 L/min in each experiment.

**2.2. Principal Component Analysis.** Principal component analysis (PCA) was used to evaluate similarities and dissimilarities within the resulting data. An exhaustive description of the method used in PCA can be found in refs 29 and 30. The primary intention of PCA is to obtain an overview of the relationships within the complete data set, i.e. not

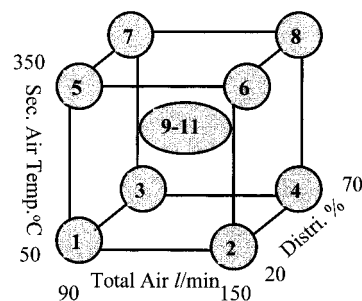


FIGURE 1. The complete factorial design (CDF) used in study and the levels of the three factors.

TABLE 1. Actual Parameter Settings in the 11 Experiments

expt	primary air (L/min)	nitrogen		sec air (L/min)	total air (L/min)	temp sec air (°C)
		flow (L/min)	total flow bed (L/min)			
1	72	60	132	18	90	50
2	120	0	120	30	150	50
3	27	60	87	63	90	50
4	45	0	45	105	150	50
5	72	60	132	18	90	350
6	120	0	120	30	150	350
7	27	60	87	63	90	350
8	45	0	45	105	150	350
9	66	30	96	54	120	200
10	66	30	96	54	120	200
11	66	30	96	54	120	200

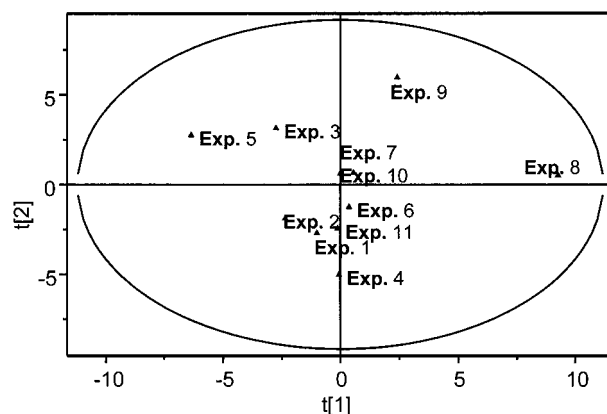


FIGURE 2. The relationship between the 11 experiments are shown in this Score plot. This figure shows the first versus the second components from the PCA. The  $R^2$  value for PC 1 and PC 2 is 0.37 and 0.25, respectively. For identification of the experiments see Table 1.

focus on one experiment at a time. The data set are divided into *objects* (here; experiments) and measured *variables* (here; concentrations of different OMPs). The *variables* are used to characterize the *objects*, e.g. the unique level of CDD/Fs and CO in the flue gas for each experiment. The results of the PCA are visualized by two figures, a so-called *score plot* and a *loading plot*. Experiments (*objects*) with similar OMP emissions will be located close to each other in the *score plot*, while those which have a divergent emission pattern will be located further apart (Figure 2). The *loading plot* shows how the measured variables relate to each other (Figure 3). Variables close to each other in the *loading plot* correlate and variables diagonally from each other have a negative correlation to each other (e.g. O<sub>2</sub> and CO). The most important variables for the PCA model are located far from the origin, and the insignificant variables are positioned close to the origin in the *loading plot*. Since the variables characterize the objects, it is possible to establish which variables (here;

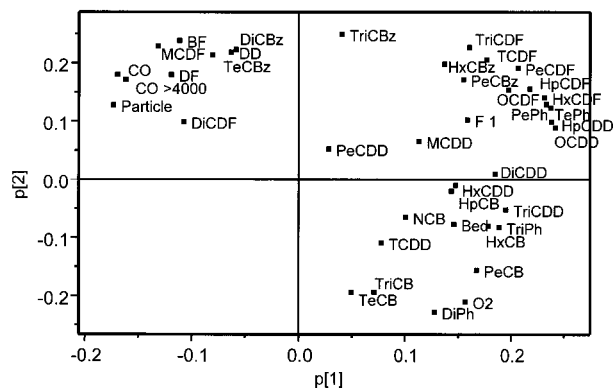


FIGURE 3. The corresponding *Loading plot* from the PCA. The variations in OMP emissions within the 11 experiments are shown in this figure. For identification of variables, see Tables 2 and 3.

TABLE 2. Measurements during the OMPs Sampling Time

expt	O <sub>2</sub> (%)	CO <sub>2</sub> (%)	CO (ppm)	CO peak <sup>a</sup> >4000 ppm	particle (mg/nm <sup>3</sup> )	THC <sup>c</sup> (ppm)	CE <sup>d</sup> (%)	Bed (°C)	F1 (°C)
1	6.2	9.6	2000	30	NS <sup>b</sup>	130	98.13	785	839
2	9.1	11	620	13	850	6.3	99.16	794	821
3	2.1	13	3000	30	930	370	97.63	689	945
4	10	9.5	190	0	590	9.6	99.70	808	834
5	2.3	9.8	3200	110	1400	340	96.37	686	872
6	8.6	10.9	520	11	850	7.3	99.17	839	859
7	6.4	7.2	750	16	690	27	98.71	658	861
8	10	10	19	0	610	0	99.94	839	920
9	5.3	9.7	1500	37	820	33	97.54	820	905
10	4.4	13	1800	33	NS <sup>b</sup>	27	97.66	731	877
11	6.5	11	200	1	790	5	99.51	722	873

<sup>a</sup> Number of CO peak above 4000 ppm during the flue gas sample period. <sup>b</sup> No sample. <sup>c</sup> Calculated as ppm hexane. <sup>d</sup> CE (%) = CO<sub>2</sub> / (CO<sub>2</sub> + CO) × 100.

homologue concentration) are responsible for the separation of the experiments in the *score plot* by examining the *loading plot*. Prior to the PCA, the data were scaled to a unit variance and mean-centered. Cross-validation was used to calculate the number of principal components (PC) to be included to provide a significantly valid model. The eigenvalue for a component has to be larger than 2 to be a significant component. The total fraction of the systematic variation in the data explained by the model is expressed as a  $R^2$  value and the fraction that can be predicted by a  $Q^2$  value. The validity of a model is decided by the  $R^2$  and  $Q^2$  value (<1.0).

### 3. Results and Discussions

**3.1. Variation in Temperatures and Combustion Gas Emissions.** The average levels of O<sub>2</sub>, CO<sub>2</sub>, CO, particulate matter, THC, temperature of the bed (Bed) and freeboard 1 (F1), and the calculated CE in each experiment are listed in Table 2. The temperature measurement of freeboard 1 is placed 350 mm above the bottom of the reactor. The level is calculated as an average value during the sampling period of OMPs. The CE in the 11 experiments has a rather large variation, between 96.37 and 99.94%, which corresponding to a variation in CO is between 19 and 3200 ppm. "High" CE is here defined as more effective than 99%, while lesser than 98% is regarded as "low" CE. Four of the 11 experiments, viz. 2, 4, 6, and 8, were performed during excess air conditions (total airflow of 150 L/min). The CE in these experiments varies between 99.16 and 99.94%, which is regarded as high CE. Experiments 4 and 8 were performed at very good combustion conditions; the CE in these two experiments are the highest, and the formation of particles and THC is consequently very low. Two of the three central experiments were performed during low CE; experiment 9 has in fact the

second lowest CE of all the experiments. Disturbances in the feeding system in this experiment cause large variation in the bed temperature (between 770 and 900 °C), which induced disturbance in the fluidization of the bed. The fluidized condition in this experiment was also negatively affected by an interruption in the external N<sub>2</sub>-flow in the bed. The inefficient fluidization conditions in this experiment cause low CE (97.54%) and high emissions of OMPs (Table 3). Experiments 1, 3, 5, and 7 were all performed during starved air-conditions (90 L/min). Two of these experiments, viz. 3 and 5, were performed at very inefficient combustion conditions. The average CO and THCs emissions in these experiments are higher than 3000 and 300 ppm, respectively, and the particulate matter in the flue gas is significant higher in these two experiments compared to the other experiments. The difference in particulate matter levels within the experiments was induced by more or less combusted particles due to different combustion conditions. A positive correlation between the ratio of total bed flow/secondary air and the particulate matter can be noticed in our data ( $R^2 = 0.80$ ). This correlation and the unexpected high CE (98.71%) in experiment 7 shows that the combustion condition was improved by preheated high secondary airflow, i.e. efficient *secondary oxidization*. Calculations showed that the bed temperature variation between the experiments was only influenced by the primary air flow in the bed and not by the total flow in the bed, i.e. the added N<sub>2</sub> has no cooling effect. High freeboard 1 temperatures were associated with high secondary, preheated air, resulting in efficient secondary oxidization and high CE.

**3.2. Emission of Organic Micropollutants and Their Correlation to Variation in Combustion Efficiency.** Table 3 shows the homologue levels of the OMPs in the 11 samples taken at various combustion conditions. The data were statistically evaluated with PCA to examine the composition of OMPs formed at different combustion conditions. The matrix contains 40 variables, including all combustion related variables such as the levels of O<sub>2</sub>, CO, and OMPs in the flue gas during the sampling time. A four component model explained 80% ( $R^2 = 0.80$ ) of the variance within the data; the remaining variance (20%) does not contain any scientifically significant information, it is the bias in the data set. The first principal component describes most of the variation within the data 37%, and the other three components PC2, PC3, and PC4 describe 25, 11, and 8.5%, respectively. The corresponding  $Q^2$  value was 0.26. Every experiment in the data set was performed at unique conditions, i.e. every experiment in the complete factorial design was important for the model (Figure 1). When every experiment in the data set is unique, it is difficult for the model to predict the particular experiment, consequently the calculated  $Q^2$ -value for the model is low. A plot of the first versus the second score vector is shown in Figure 2 (*score plot*) which shows the relationship between the 11 experiments, due to their differences in OMP formation. The corresponding loading vectors are shown in the *loading plot* (Figure 3). A general trend in the *score plot* is that experiments performed at inefficient conditions with high emissions of CO, THCs, and particles are placed in the upper left-hand side of the plot, while the experiments performed with efficient combustion conditions are placed more to the right side in the plot. As can be seen in Figure 2, experiments 5 and 8 and 9 and 4 are the most important in PC1 and PC2, respectively. Thus, these four experiments showed the largest variations in emission pattern. Although these experiments have high influence on the PCA and the resulting *score plot*, the relation between the experiments remained unchanged in models excluding any of these four experiments. The *loading plot* (Figure 3) shows the characteristic homologue pattern in each experiment, i.e. how the concentration level of the OMP homo-

TABLE 3. OMPs Levels in Each Flue Gas Sample<sup>a</sup>

	1	2	3	4	5	6	7	8	9	10	11
DF ( $\times 10^3$ )	403	158	104	41.0	1120	83.1	19.7	1.50	751	377	9.80
MCDF	103	68.6	173	10.0	282	27.8	48.7	3.87	232	4.78	9.34
DiCDF	32.6	19.3	74.9	0.01	82.1	0.00	66.3	30.1	0.02	0.01	35.1
TriCDF	10.5	7.88	19.0	3.08	11.6	19.3	26.7	31.1	38.5	17.0	18.0
TCDF	19.3	9.00	60.3	8.48	13.8	21.9	45.3	84.1	72.4	54.4	32.5
PeCDF	16.5	12.0	54.8	10.4	10.2	32.7	50.3	115	101	54.2	31.8
HxCDF	11.1	11.8	22.0	7.26	6.35	31.3	42.0	119	80.8	36.7	23.3
HpCDF	6.55	8.05	4.42	4.91	2.18	16.4	25.4	75.6	72.1	22.8	12.7
OCDF	3.94	3.83	1.01	3.60	0.73	6.38	10.5	16.0	21.2	7.29	3.05
DD	13.8	28.8	15.7	28.0	183	29.0	0.50	13.8	203	67.6	2.60
MCDD	0.87	0.40	3.83	0.02	0.01	1.17	0.05	4.08	0.06	3.05	0.47
DiCDD	4.63	0.06	5.74	0.11	0.07	1.53	0.32	15.9	0.20	2.85	3.56
TriCDD	3.94	0.13	1.10	1.23	0.27	1.47	0.05	9.20	0.87	3.37	4.37
TCDD	19.8	2.82	6.83	7.90	2.38	6.89	17.0	11.1	4.10	5.70	9.06
PeCDD	16.3	10.1	24.1	14.3	10.3	8.31	53.3	16.4	17.2	7.13	15.4
HxCDD	15.8	8.52	12.9	13.8	2.84	15.4	29.9	20.2	16.4	5.55	13.9
HpCDD	2.90	3.76	2.71	2.83	0.91	6.01	7.96	18.9	13.0	3.32	5.94
OCDD	1.49	1.73	0.95	1.58	0.31	2.56	4.29	10.3	6.00	2.07	1.71
BP ( $\times 10^3$ )	16.3	46.6	596	106	807	287	49.8	7.09	630	361	6.8
TriCB	628	33	124	485	72	22	59	400	47	121	429
TeCB	508	9.61	10.1	3110	11.1	14.5	20.2	806	20.6	18.3	394
PeCB	25.2	3.28	4.40	48.4	5.60	9.34	7.50	64.3	7.29	6.40	44.2
HxCB	12.8	6.83	8.40	26.5	12.6	16.9	18.0	27.9	14.4	19.0	12.1
HpCB	0.00	5.69	6.07	27.4	7.10	12.5	11.0	27.3	12.2	26.2	0.00
NCB	0.00	1.38	0.00	0.00	0.42	2.21	0.00	0.00	2.46	0.03	0.00
DCB	0.00	0.97	0.00	0.00	0.41	0.75	0.00	0.00	0.74	0.00	0.00
DiCPh	5.75	3.68	1.60	9.84	1.20	3.63	1.39	7.66	2.33	3.33	4.99
TriCPh	3.55	2.62	1.37	2.27	0.73	4.62	1.66	6.18	2.28	5.19	3.34
TeCPh	1.12	0.58	1.37	0.67	0.29	1.27	1.72	5.24	3.43	1.61	1.39
PeCPh	0.32	0.24	0.31	0.27	0.13	0.57	1.10	2.24	1.59	0.86	0.45
DiCBz	1.04	0.53	10.6	0.57	3.80	0.50	1.46	1.67	5.25	0.76	0.72
TriCBz	0.71	0.45	5.67	0.63	0.91	1.26	1.54	1.89	7.59	0.93	1.31
TeCBz	0.06	0.20	2.56	0.18	0.78	0.10	0.81	0.07	1.06	0.58	0.02
PeCBz	0.42	0.79	0.23	0.39	0.57	1.79	1.71	2.25	3.75	0.37	0.55
HxCBz	0.06	0.09	0.05	0.05	0.23	0.17	0.16	0.37	NA <sup>b</sup>	0.25	0.04

<sup>a</sup> CDD/Fs and CBs ng/nm<sup>3</sup>, CPhs and CBzs  $\mu\text{g}/\text{nm}^3$ . <sup>b</sup> Not analyzed due to disturbance in the analysis.

logues shifts within the 11 experiments. The overarching difference due to variation in combustion conditions is more correlated to the degree of chlorination of the OMPs than to what kind of OMPs (e.g. CBzs, CDF, or CPh) that are formed. The lower chlorinated homologues are generally formed in higher levels during inefficient combustion conditions and consequently placed in the upper left corner of the plot, close to the variables CO and particulate matter which are well-known as indicators of inefficient combustion. The degree of chlorination increases toward the right-hand side of the plot, where the O<sub>2</sub> variable also is placed. Experiments 3, 5, and 9 are all performed with low CE, and their emissions of the nonchlorinated and the lower chlorinated homologues are 5–10 times higher than for the experiments performed during high CE. In the *loading plot* a correlation between the BP, DD, DF, MCDFs, DiCDFs, and di- to tetraCBzs and the levels of particles, CO, and number of CO peaks in the combustion gas can be noticed (Figure 3). The nonchlorinated DD, DF, and BP can be considered as small PAHs, and a correlation between high CO levels and high PAH emissions in combustion gases has been reported by others (4, 5). The level of DF is 1 order of magnitude higher than the DD. By the rule of Hückel the DF molecule is defined as an aromatic compound, i.e. stabilized by delocalized electrons, while the DD is not. The difference in stability can be one of the reasons for the difference in formation. At inefficient combustion condition, the MCDF and DiCDF homologues clearly dominate the CDF profile. This can be seen in experiment 5 which has very high CDF levels and very inefficient combustion. The highest CO, THC, and particulate matter formation was noticed in this experiment also. About 80% of the mono- to octaCDFs in this experiment remain from the MCDF and

DiCDF isomers. The MCDF and DiCDF homologues dominate in all of the three experiments (3, 5, and 9). The average homologue pattern consisted of approximately 60% MCDF and DiCDF. As can be seen in the *loading plot* the homologue profile of the CBzs also are effected by variations in combustion conditions. More than 75% of the CBzs are present as di- and triCBzs when the experiments are performed at inefficient combustion. Changes within the CDD homologue profile are not as influenced as the CDF and the CBz due to variations in the combustion conditions. The levels of mono- to triCDDs are very low compared to the other OMP homologues in their flue gas, and the formation is not affected systematically by variations in combustion efficiency. The only experiment that has a distinct formation of the mono- to triCDDs is experiment 8 which was performed with very efficient combustion condition. However, the penta- and hexaCDD homologues are the dominant homologue in all experiments, independent of variation in combustion conditions. A general CB homologue profile within these experiments independent of variations in combustion conditions is also noticed (TriCB > TeCB > HxCB > HpCB > PeCB > NCB > DCB). The levels of the studied CB homologues vary greatly within the 11 experiments, between 3000 and a few ng/nm<sup>3</sup>. The PCA showed that CB formation highly correlates to excess air condition, contrary to the biphenyl which is formed at inefficient combustion conditions. Table 3 shows that the levels of tri- and tetraCBs are more affected by variations in combustion conditions than the higher chlorinated homologues. Experiments 4, 8, and 11 are all performed with a CE higher than 99.50%, and the formation of THCs and particles are relatively low. The formation of tri- and tetraCBs in these three experiments are

very high as well. It seems that the formation of the lower CBs are controlled by different parameters (mechanisms) than the higher CBs and/or that they can act as precursors for the formation of higher CBs. As can be seen in the *loading plot*, the CPh formation, particularly the di- and triCPh homologues, is distinctly influenced by the amount of air in the system. The lowest formation of CPhs is found in experiments 3, 5, 7, and 9 which all were performed at relatively inefficient combustion. Experiments 4 and 8, performed with the highest combustion efficiency, have significantly higher levels of CPhs formed than the other experiments. Consequently, the two variables di- and triCPh are placed in the lower right corner of the *loading plot*, very close to the O<sub>2</sub> variables and opposite the CO variables. The levels of tetra- to octaCDD/Fs, tetra- to pentaCPhs, and penta- to hexaCBzs are generally higher in samples taken from experiments 7–11. All these experiments were performed at different total amounts of air but all had high preheated secondary airflow, i.e. performed at efficient secondary oxidization. These homologues are placed in the upper right corner of the *loading plot*. This shows that the total amount of air is not the only important parameter for the formation of these higher chlorinated homologues. How the air is distributed between the primary and secondary is also important, i.e. at efficient secondary oxidization the formation increase. The importance of efficient secondary oxidization in reducing the amount of formed OMPs has been shown in other studies (3, 31). A difference between these studies and our study is that their samples are taken after the ESP or after the boiler at a temperature around 200–300 °C, i.e. after both primary and secondary formation, while our study only is discussing the primary formation at high temperature. Oxygen is essential in the formation process of chlorinated OMPs in three ways: the chlorination reactions through Deacon mechanism, the oxidative breakdown of carbon on the surface of the fly ash (de Novo synthesis), and in the chlorination reaction of aromatics by CuCl<sub>2</sub> (32–37). During incomplete combustion at high temperatures, most of the reactions involve H, OH, O, and O<sub>2</sub>H radicals. Cui et al. (38) suggested that chlorination reactions are unfavored when H atoms are present in the combustion gas, and Hagenmaier et al. (14) suggest that fly ash catalyze dechlorination/hydrogenation reactions if the reactions occur during starved air conditions. Their results also indicate that the CDD/F formation increased during oxygen surplus conditions, a correlation that first was described by Vogg and Stieglitz (15). The present of H-atoms and the low levels of oxygen in the flue gas can be two of the reasons for the low formation of higher chlorinated homologues during the experiments performed at inefficient combustion conditions. An explanation of the high formation at high *secondary oxidization* conditions could be that the Deacon reaction is enhanced by the high oxygen level in the flue gas. The only conditions in which the higher chlorinated OMPs (Cl > 4) can be formed or chlorinated is during efficient *secondary oxidization* conditions due to the oxygen-demanding chlorination reactions. These results show that there is a complex correlation between the oxidization reactions and the formation of chlorinated OMPs.

**3.3. Congener Distribution of the CDD and CDF in the Flue Gas.** The congener patterns and homologue profiles were closely evaluated to enhance the understanding of any similarities or dissimilarities in the CDD and CDF formations. The levels of each homologue group changed due to differences in combustion conditions, while the congener distribution patterns were more or less the same, independent of variations in the combustion conditions. Table 4 lists the dominating isomers and their percentage part in each homologue group. Almost all of the 135 congeners of the mono- to octaCDF are formed during primary formation, except a few di- and triCDF isomers. The extensive formation

TABLE 4. Dominating CDD/F Isomers in Each Homologue Presented in Percentage of the Homologue<sup>a</sup>

homologue	CDDs	%	CDFs	%
mono	2-	40	2-	60
di	[23-,28-]		no particular	30
tri	138-	20	[234-,238-,237-]	30
tetra	1368-	15	[1234-,2349-]	40
penta	[12468-,12479-]	15	23467-	50
hexa	[124679-,123468-,124689-]	20	123467-	70
hepta	50/50 of the two HpCDDs	40	1234678-	

<sup>a</sup> [-]: coeluating isomers. The mono-, di-, and triCDD are only formed in experiment 8.

of almost all congeners show that the dibenzofuran is formed through non- or low-chlorinated precursors, followed by further chlorination to form the CDFs. A more selective congener formation would have been expected if the CDFs were formed from chlorinated precursors. Chlorination experiments of DF and/or DD have been performed by Luijk et al. (18) and Addink et al. (39) in microscale quartz reactor systems. These experiments show that majority of the CDDs/CDFs were present as octaCDD/octaCDF and that the lateral positions (2, 3, 7, 8) were preferred for chlorination, i.e. the law of electrophilic aromatic substitution was followed. Such a CDD/F pattern is normally not found in flue gas samples from normal MSW combustion processes and so is also the case in our study. A reason for the disagreement in the congener pattern between microscale laboratory results, and real flue gas samples can be the distinction between the conditions in the systems. Many reactions other than the specific chlorination reactions ruled by electrophilic aromatic substitution are very likely to occur in complex combustion systems. The congener pattern and homologue profile in flue gas samples taken from different MSW incinerators is quite constant, independent of variations in combustion conditions. The stable pattern implies that the formation could be controlled by thermodynamic properties. The 2,3,7,8-substituted CDD congeners have been shown to be more thermodynamically stable than the 1,4,6,9-substituted (40–42). However, the thermodynamically controlled model is not able to entirely explain the stable extensive congener pattern in the flue gas from MSW incineration. Therefore, contributions of other mechanisms had to be included in the formation. The relative activity, i.e. the differences in frontier orbital (HOMO and LUMO) for all CDD congeners, was calculated by Wehrmeier et al. (43). The 2,3,7,8-substituted congeners were shown to be more sensitive for oxidative/reductive breakdown than the other congeners, and the most stable congeners were the 1,4,6,9-substituted. Considering this unstability of the most thermodynamic stable congeners, the calculated most probable congener pattern according to the law of thermodynamic will shift. A pattern where the congeners with chlorine substituted in position 1,4,6,9 has a larger importance. A combination of chlorination/dechlorination (formation/destruction) reactions of the CDF congeners may explain the extensive congener distribution found in our experiments.

The similarity in substitution pattern of the tetra- to heptaisomers in our data shows that the formation mechanism can be the same, formed by the same precursor or by the same chlorination reactions of the lower chlorinated CDF homologues. Only half of the 75 CDD congeners are formed during primary CDD formation. The extensive congener formation found for the CDFs is not noticed. The 1,3,6,8- and 1,3,7,9-TCDD isomers constitute for 50 and 20%, respectively, of the TCDD pattern. These two TCDD isomers are well-known as products from condensation of two 2,4,6-triCPh. The same can be noticed within the PeCDDs, approximately 50% origin from the two coeluating isomers

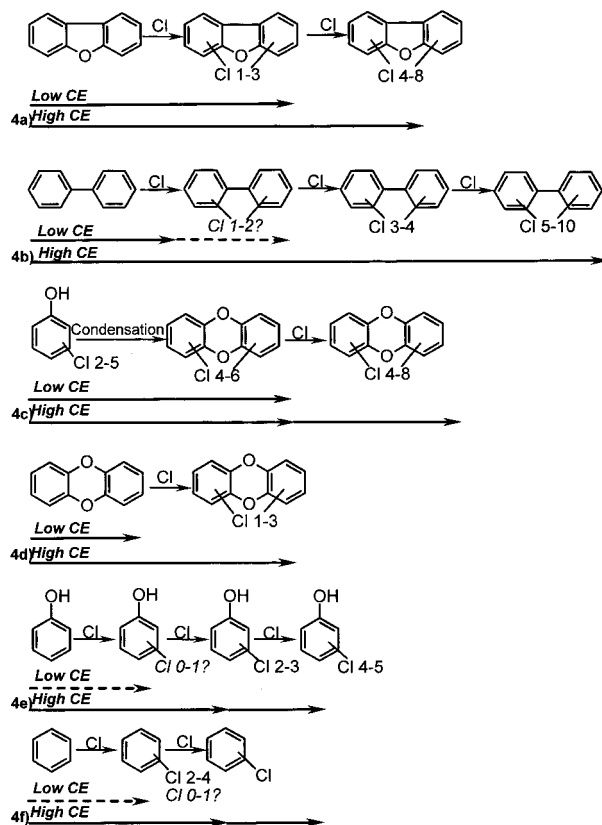


FIGURE 4. A general picture of the dominating reactions at efficient and inefficient combustion conditions. The OMP levels are compared as relative OMP levels, to focus on differences in dominating reaction and not the changes in levels.

[1,2,4,6,8-1,2,4,7,9]-PeCDD and additional 15% origin from the 1,2,3,6,8-PeCDD isomer. The dominating Pe- and HxCDD isomers are substituted very much like the two TCDD isomers. Possible formation mechanisms are by further chlorination of the TCDDs or by condensation reactions of tetra- and pentaCPh isomers. The importance of the CPh condensation in microscale experiments has been shown in many studies before (10, 18, 44). Our data confirm that CDD formation through CPh condensation is a very important formation mechanism even in complex combustion processes. The selective CDD-congener formation shows that the most important formation pathway is through condensation of chlorinated precursors, such as CPhs. Further, the formation of CDDs in our experiments is not influenced by variations in the combustion conditions. One of the reasons for this independence could be that the major formation mechanism (condensation of CPhs) can operate independently of changes in oxidization conditions (16, 17). The dominating CDD/F congeners in our experiments agree very well with the most favored congeners in well-controlled quartz reactor experiments. The stable and unchanged dominant congener pattern indicates that local equilibrium and steady-state conditions are obtained in the flue gas.

Generally, two markedly different combustion situations can be distinguished, an efficient and an inefficient combustion. At high oxygen levels, i.e. at efficient combustion condition, the Deacon reaction is favored, and the chlorine in the flue gas is more available. At inefficient combustion the levels of chlorination inhibitors, such as H atoms, is higher, and the chlorination reaction is limited. Figure 4 summarizes the formation pathways of the OMPs that dominate during efficient and inefficient combustion conditions. To focus on the changes in pattern and not the changes in formation, the homologue levels within the experiments

are compared as relative levels. The DF is predominantly formed at inefficient combustion conditions (see Figure 4a). The chlorinated homologues are then formed after further chlorination of the DF, which is verified by the extensive CDF congener formation. The degree of chlorination is then controlled by the efficiency of the combustion conditions. Higher chlorinated homologues are formed during efficient oxidization condition. The same relationship can be seen for the biphenyls (Figure 4b). Experiments performed with inefficient combustion conditions have high biphenyl emission and at the same time relative low formation of chlorinated biphenyls. This shows that the nonchlorinated biphenyl is formed at inefficient combustion conditions, while the CBs are formed after further chlorination reactions of the biphenyl at efficient combustion. The most probable formation pathway for the CDDs is through condensation reactions of two CPhs, a reaction that operates independently of variations in combustion conditions (Figure 4c). The efficiency of the combustion process is then controlling the further chlorination reactions. The DD is predominantly formed at inefficient combustion. If the combustion condition is efficient, the DD can be further chlorinated into lower CDDs (Figure 4d). The CPhs are generally formed at efficient combustion; the degree of chlorination increases with increasing CE (Figure 4e). However, how the phenol and the MCPH is effected by the combustion conditions cannot be concluded from our data, but most probably the phenol is formed at high levels when the combustion is inefficient. The relationship found for the formation of CPhs at different combustion conditions is the same as for the CBzs (Figure 4f). The degree of chlorination is controlled by the combustion efficiency. One important step in the aromatic ring-breaking reactions of a benzene during high temperature reactions is the formation of a phenyl radical. This radical is then very likely converted into a phenol or into smaller hydrocarbons (45). Thus, the benzene molecule can be a very important precursor for formation of phenols and probably also for the BP, the DF, and the DD.

## Acknowledgments

The author thanks the TFR (Swedish Research Council for Engineering Sciences, (*In Swedish: Teknikvetenskapliga Forskningsrådet*)) and Norsk Hydro AB for financial support of the study. Special thanks to Per Liljelind, Gunilla Söderström, Lisa Börjeson, Gunilla Löfvenius, and Maria Hjelt at the Environmental Chemistry for all their help with the combustion experiments, laboratory work, and fruitful discussions.

## Literature Cited

- (1) Hasselriis, F. *Waste Manage. Res.* **1987**, *5*, 311.
- (2) Bergström, J.; Warman, K. *Waste Manage. Res.* **1987**, *5*, 395.
- (3) Takeshita, R.; Akimoto, Y.; Nito, S.; Nishigaki, M.; Kawashima, M. *Organohalogen Compd.* **1990**, *3*, 183.
- (4) Oehme, M.; Mano, S.; Mikalsen, A. *Chemosphere* **1987**, *16*, 143.
- (5) Benestad, C.; Hagen, I.; Jebens, A.; Oehme, M.; Ramdahl, T. *Waste Manage. Res.* **1990**, *8*, 193.
- (6) Lenoir, D.; Kaune, A.; Hutzinger, O.; Muetzenich, G.; Horch, K. *Chemosphere* **1991**, *23*, 1491.
- (7) Commoner, B.; Webster, T.; Shapiro, K.; McNamara, M. *Proc.-APCA Annu. Meet.* **1985**, *78*, 1.
- (8) Sakai, S.; Hiraoka, M.; Takeda, N.; Shiozaki, K. *Chemosphere* **1996**, *32*, (1), 79.
- (9) Nottrodt, A.; Duetzel, U.; Ballschmiter, K. *Chemosphere* **1990**, *20*, 1847.
- (10) Born, J. G. P.; Mulder, P.; Louw, R. *Environ. Sci. Technol.* **1993**, *27*, 1849.
- (11) Andersson, P.; Marklund, S. *Chemosphere* **1998**, *36*, (6), 1429.
- (12) Crummett, W. B.; Townsend, D. I. *Chemosphere* **1984**, *13*, 777.
- (13) Eiceman, G. A.; Rghei, H. O. *Chemosphere* **1982**, *11*, 833.
- (14) Hagenmaier, H.-P.; Kraft, M.; Brunner, H.; Haag, R. *Environ. Sci. Technol.* **1987**, *21*, 1080.
- (15) Vogg, H.; Stieglitz, L. *Chemosphere* **1986**, *15*, 1373.

- (16) Dickson, L. C.; Lenoir, D.; Hutzinger, O. *Environ. Sci. Technol.* **1992**, *26*, 1822.
- (17) Dickson, L. C.; Karasek, F. W. *J. Chromatogr.* **1987**, *389*, 127.
- (18) Luijk, R.; Akkerman, D. M.; Slot, P.; Olie, K.; Kapteijn, F. *Environ. Sci. Technol.* **1994**, *28*, 312.
- (19) Altwicker, E. R. *Chemosphere* **1996**, *33*(10), 1897.
- (20) Huang, H.; Buekens, A. *Chemosphere* **1995**, *31*(9), 4099.
- (21) Hell, K.; Stieglitz, L.; Zwick, G.; Will, R. *Organohalogen Compd.* **1997**, *31*, 492.
- (22) Wikström, E.; Marklund, S. *Waste Manage. Res.* **1998**, *16*(4), 342.
- (23) Wikström, E.; Andersson, P.; Marklund, S. *Rev. Scientific Instruments* **1998**, *69*(4), 1850.
- (24) Marklund, S.; Söderström, G.; Ljung, K.; Rappe, C.; Kraft, M.; Hagenmaier, H.-P. *Waste Manage. Res.* **1992**, *10*, 21.
- (25) European Standard *EN 1948: 1-3* **1997**.
- (26) van Bavel, B.; Fängmark, I. E.; Marklund, S.; Söderström, G.; Ljung, K.; Rappe, C. *Organohalogen Compd.* **1992**, *8*, 225.
- (27) Marklund, S. Ph.D. Thesis Environmental Chemistry, Umeå University, Umeå, Sweden, 1990.
- (28) Wold, S.; Sjöström, M.; Carlsson, R.; Lundstedt, T.; Hellberg, S.; Skagerberg, B.; Wikström, C.; Öhman, J. *Anal. Chim. Acta* **1986**, *191*, 17.
- (29) Jackson J. E. *A user Guide to Principal Components*; Wiley: 1991.
- (30) Jolliffe I. T. *Principal Component Analysis*; 1986.
- (31) Ishikawa, R.; Buekens, A.; Huang, H.; Watanabe, K. *Chemosphere* **1997**, *35*(3), 465.
- (32) Stieglitz, L.; Bautz, H.; Zwick, G.; Will, R.; Schild, D.; Romer, J. *Organohalogen Compd.* **1996**, *27*, 5.
- (33) Griffin, R. D. *Chemosphere* **1986**, *15*, 1987.
- (34) Benfenati, E.; Mariani, G.; Fanelli, R.; Farneti, A. *Chemosphere* **1991**, *23*, 715.
- (35) Tong, H. Y.; Karasek, F. W. *Chemosphere* **1986**, *15*, 1219.
- (36) Addink, R.; Olie, K. *Environ. Sci. Technol.* **1995**, *29*(6), 1586.
- (37) Stieglitz, L.; Vogg, H. *Chemosphere* **1987**, *16*, 1917.
- (38) Cui, J. P.; He, Y. Z.; Sang, W. *J. Phys. Chem.* **1989**, *93*, 724.
- (39) Addink, R.; Paulus, R. H. W. L.; Olie, K. *Environ. Sci. Technol.* **1996**, *30*(7), 2350.
- (40) Thompson, D. *Chemosphere* **1994**, *29*(12), 2545.
- (41) Thompson, D. *Chemosphere* **1994**, *29*(12), 2583.
- (42) Unsworth, J. F.; Dorans, H. *Chemosphere* **1993**, *27*, 351.
- (43) Wehrmeier, A.; Lenoir, D.; Schramm, K.-W.; Zimmerman, R.; Hahn, K.; Henkelmann, B.; Kettrup, A. *Chemosphere* **1998**, *36*(13), 2775.
- (44) Ballschmiter, K.; Braunmiller, I.; Niemczyk, R.; Swerev, M. *Chemosphere* **1988**, *17*, 995.
- (45) Emdee, J. L.; Brezinsky, K.; Glassman, I. *Phys. Chem.* **1992**, *96*, 2151.

Received for review May 18, 1999. Revised manuscript received August 31, 1999. Accepted September 14, 1999.

ES990568B